

## **Spin-Precession Organic Magnetic Sensor**

SRI Project P19028

ONR Contract N00014-09-C-0292

Prepared by:

Srini Krishnamurthy, Senior Principal Scientist  
Applied Physical Sciences Laboratory

Prepared for:

Office of Naval Research  
Code 321MS  
875 N. Randolph Street  
Arlington VA 22203-1995  
Attention: Leroy Sverduk

DISTRIBUTION STATEMENT A

Report Documentation Page			Form Approved OMB No. 0704-0188		
Public reporting burden for the collection of information is estimated to average 1 hour per response, including the time for reviewing instructions, searching existing data sources, gathering and maintaining the data needed, and completing and reviewing the collection of information. Send comments regarding this burden estimate or any other aspect of this collection of information, including suggestions for reducing this burden, to Washington Headquarters Services, Directorate for Information Operations and Reports, 1215 Jefferson Davis Highway, Suite 1204, Arlington VA 22202-4302. Respondents should be aware that notwithstanding any other provision of law, no person shall be subject to a penalty for failing to comply with a collection of information if it does not display a currently valid OMB control number.					
1. REPORT DATE <b>JUN 2011</b>		2. REPORT TYPE		3. DATES COVERED <b>00-00-2011 to 00-00-2011</b>	
4. TITLE AND SUBTITLE <b>Spin-Precession Organic Magnetic Sensor</b>			5a. CONTRACT NUMBER		
			5b. GRANT NUMBER		
			5c. PROGRAM ELEMENT NUMBER		
6. AUTHOR(S)			5d. PROJECT NUMBER		
			5e. TASK NUMBER		
			5f. WORK UNIT NUMBER		
7. PERFORMING ORGANIZATION NAME(S) AND ADDRESS(ES) <b>SRI International,333 Ravenswood Avenue,Menlo Park,CA,94025</b>			8. PERFORMING ORGANIZATION REPORT NUMBER		
9. SPONSORING/MONITORING AGENCY NAME(S) AND ADDRESS(ES)			10. SPONSOR/MONITOR'S ACRONYM(S)		
			11. SPONSOR/MONITOR'S REPORT NUMBER(S)		
12. DISTRIBUTION/AVAILABILITY STATEMENT <b>Approved for public release; distribution unlimited</b>					
13. SUPPLEMENTARY NOTES					
14. ABSTRACT					
15. SUBJECT TERMS					
16. SECURITY CLASSIFICATION OF:			17. LIMITATION OF ABSTRACT <b>Same as Report (SAR)</b>	18. NUMBER OF PAGES <b>12</b>	19a. NAME OF RESPONSIBLE PERSON
a. REPORT <b>unclassified</b>	b. ABSTRACT <b>unclassified</b>	c. THIS PAGE <b>unclassified</b>			

## CONTENTS

EXECUTIVE SUMMARY .....	2
TECHNICAL DISCUSSION .....	3
1. Objectives .....	3
2. Device Concept, Operation, and Approach .....	3
3. Device Design and Fabrication .....	3
4. Local Devices and Results .....	4
5. Nonlocal CFAS Devices and Results .....	7
6. Conclusions .....	10

## EXECUTIVE SUMMARY

This report consists of two parts—results from  $\text{La}_{0.7}\text{Sr}_{0.3}\text{MnO}_3$  (LSMO) studies carried out in collaboration with the University of Delaware (UD) and the University of California at Riverside (UCR); and results from  $\text{CoFe}_{50}\text{Al}_{25}\text{Si}_{25}$  (CFAS) studies carried out in collaboration with Arizona State University (ASU)—both conducted under ONR Contract (N00014-09-C-0292). The objective of the project is to develop an ultrasensitive magnetic sensor for room temperature operation. The requirements are (a) half-metallic ferromagnetic contacts with high Curie temperature,  $T_c$  and (b) polymer with very long spin lifetimes. Previously under this program we demonstrated (a) growth of high-quality LSMO with critical temperature  $T_c \sim 360$  K and metal-semiconductor transition temperature,  $T_{MS} > 400$  K; (b) charge and spin injection from LSMO into low-mobility polymers; and (c) high magnetoresistance (MR) in micron-thick polymer devices. The results of this study were published in *Applied Physics Letters*.

In the first part of this year (June 2010 to September 2010), we fabricated several devices with LSMO and polymer (P3HT) and evaluated the magnetic sensor operation. While spin precession, a requirement for ultra-high sensitivity, could be observed at low temperature, the device performance at room temperature was dominated by noise. The cause of increased noise is the associated decrease in contract magnetization. Since LSMO has a  $T_c$  that is only slightly higher than room temperature, the magnetization at room temperature is very small, thus reducing the signal. In our local device where both current and voltage are measured between the same two terminals, the resistance changed with time, resulting in increased noise. Consequently, the signal-to-noise ratio (SNR) is too small for acceptable sensor performance.

Based on the knowledge acquired in our studies, we identified the CFAS as the half-metallic FM with very high room temperature magnetization for improved signal, and a nonlocal device design for reduced noise. We have grown CFAS by pulsed laser deposition and demonstrated its very high and temperature-*independent* magnetization ( $\sim 1000$  emu/cc), high coercive field ( $\sim 450$  Oe), low resistivity ( $\sim 50$   $\mu\Omega\text{-cm}$ ), high critical temperature ( $\sim 1000$  K), and large spin polarization ( $p \sim 0.5\text{-}0.6$ ). This report describes the results of our systematic studies.

Currently we are fabricating a nonlocal device to demonstrate spin injection and magnetic sensing. In parallel, we are developing a DC magnetron approach to grow ultra-smooth CFAS layers to possibly increase spin polarization. The results of these studies will be presented at the annual review.

## TECHNICAL DISCUSSION

### 1. Objectives

Our long-term goal is to develop an ultrasensitive, room temperature, compact magnetic sensor based on spin precession. The specific aim of this study was to fabricate a magnetic sensor device with half-metal ferromagnets (FM) as contacts and polymer as a transport medium to demonstrate and optimize the sensing capability of the device. The sensitivity depends crucially on efficiency of spin injection and duration of spin relaxation time. The half-metallicity ensures high spin injection, and the small spin-orbit interaction in polymers ensures long spin lifetimes. We consider  $\text{La}_{0.7}\text{Sr}_{0.3}\text{MnO}_3$  (LSMO) and  $\text{CoFe}_{50}\text{Al}_{25}\text{Si}_{25}$  (CFAS) as possible candidates for half-metallic FM contacts and poly(3,4-ethylenedioxythiophene) (PEDOT), poly-3(hexylthiophene) (P3HT), or poly[2-methoxy, 5-(2-ethylhexoxy)-1,4-phenylene vinylene] (MEH-PPV) as candidates for polymers.

### 2. Device Concept, Operation, and Approach

The device considered here is a planar structure that uses a half-metal such as LSMO or CFAS for the contacts and an organic material for electron transport. The contacts are magnetically poled to have magnetization parallel to each other. The half-metal nature of the contact allows injection of only one kind of spin (parallel to the magnetization) into the organic material. The constituents of the organics are usually atoms with small atomic numbers (such as H, C, N, O, and S) and the spin-orbit coupling is extremely small, which allows the injected spins to stay coherent for long times. In the absence of any magnetic field, the injected electrons will retain the spin and can find a state in the other contact when the two contact magnetizations are parallel. However, when a magnetic field is applied, the electron spin will precess and the spin orientation with respect to contact magnetization changes, resulting in an increased resistance. Since a very small magnetic field is required to alter the electron spin orientation, the device is predicted to have very high sensitivity, even in room temperature operation.

### 3. Device Design and Fabrication

We considered two classes of devices: local devices with LSMO as contacts and non-local devices with CFAS as contacts. In the local device, both current and voltage are measured across the same two terminals. The advantage of this approach is that the carrier drift is faster under external electric field and, hence, the device has a higher speed. On the flip side, the interface issues that affect the spin injection will also affect the measured signal, leading to a poorer SNR. In the nonlocal devices, a constant current is supplied between two terminals and the voltage is

measured between two other terminals. Since the injection is separated from the signal measurement, the SNR is higher. The main drawback of this class of device is that the spin diffusion (rather than a drift transport under an electric field) determines the open circuit voltage, and hence only long spin lifetimes can guarantee a measurable voltage signal.

For local *vertical* devices, our approach takes the following steps:

1. Grow high-quality LSMO layers by molecular beam epitaxy (MBE) on an ultra-flat  $\text{SrTiO}_3$  (STO) substrate.
2. Deposit a patterned metal layer to make ohmic contact to two pieces of LSMO.
3. Deposit a thin layer of P3HT in a micron-deep well on one of the LSMO pieces.
4. Place the other LSMO piece on top of P3HT layer and make a sandwich structure by tightly holding them together and thermal annealing for better contact.
5. Apply a voltage between the LSMO contacts and measure the current as a function of applied magnetic field.

For non-local *planar* devices, our approach takes the following steps:

1. Grow high-quality CFAS layers on an ultra-flat STO substrate.
2. Pattern the CFAS layers into four strips and make Au contact to each of those strips.
3. Spin-coat or drop-cast a thin layer of PEDOT (or MEH-PPV) on CFAS strips
4. Apply constant current between strips 1 and 2, and measure the voltage between strips 3 and 4 as a function of magnetic field.

#### 4. Local Devices and Results

High-quality LSMO layers were grown by Professor Jing Shi at UCR, and devices were fabricated at SRI and tested for magnetic response at UD. Several devices differing in polymer deposition, polymer anneals, polymer thickness, and polymer surface roughness were fabricated and tested. Figure 1 shows a typical device. The crossbar holds the top and bottom LSMO pieces together. The electrical contacts are connected to a chip carrier for convenience of testing and transportation. For comparison, we had also fabricated a monolithic device consisting of Co/P3HT/Co, where the top FM layer of Co is evaporated on the polymer. This device is expected to have a near-perfect interface between the polymer and the FM layers. The measured current - voltage (I-V) curves are shown in Figure 2 for the Co device and in Figure 3 for the LSMO device. We note that I-V is nearly linear in the monolithic device. The measured room temperature resistance closely matches the calculated values.

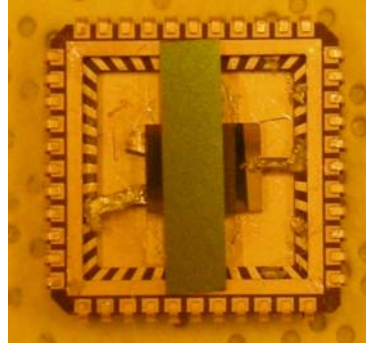


**Figure 1: Typical vertical device.**

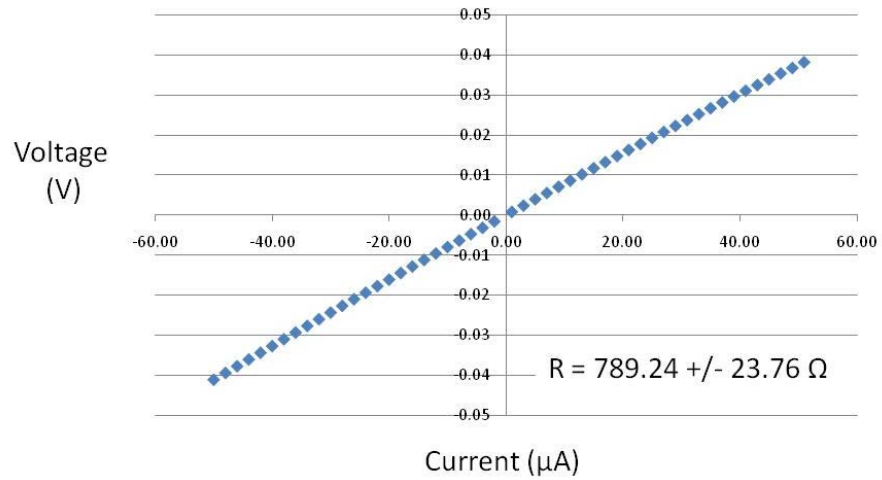


**Figure 2: Measured I-V curve for monolithic Co/P3HT/Co device.**

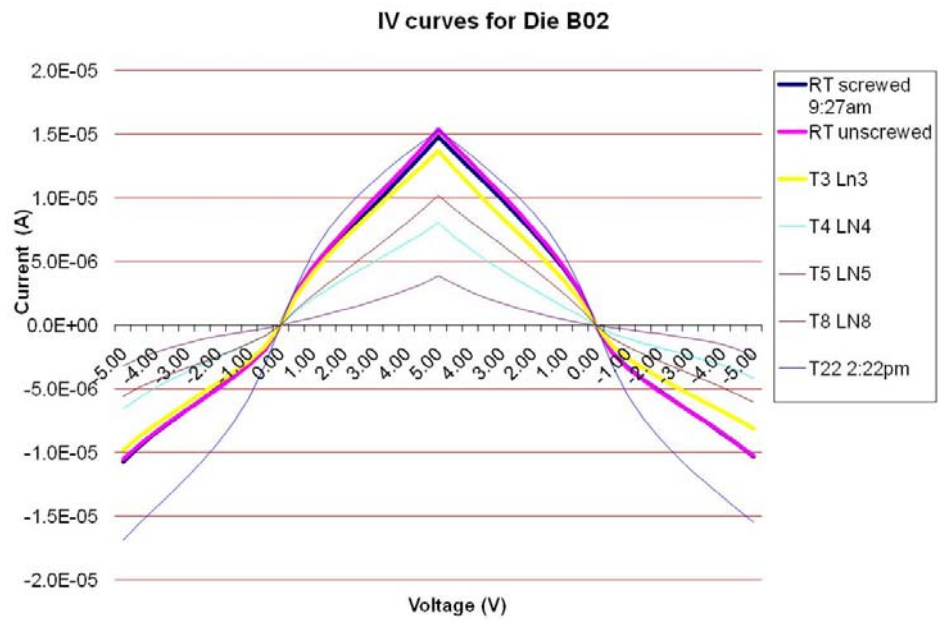


**Figure 3: Measured I-V curves from LSMO/P3HT/LSMO device.**

In the I-V curves for LSMO device shown in Figure 3, the I-V response was measured first at room temperature before and after pressing the top and bottom LSMO plates together; then at liquid nitrogen (LN) temperature of 77 K; and finally again at room temperature. As seen from Figure 3, the I-V curve changed with time when measured at 77 K, but is nearly unchanged after a thermal cycle to yield similar I-V at room temperature. However, all curves are nonlinear (i.e., resistance change with the applied bias), indicating poorer polymer/LSMO interface. When the contact is non-ohmic, the charge injection is through tunneling and the I-V curve will be nonlinear. The device was then shipped to UD for electrical and magnetic measurements. The measured resistance (R) at 1 V of bias is plotted in Figure 4 as a function of time. The value measured at SRI is shown by a red dot. The same device yielded a higher resistance at UD (denoted ‘as made-UD’) and decreased as a function of time. When that device is annealed for curing the polymer, the resistance dropped, but continued to decrease (denoted as ‘cured-UD’) with time. Finally, the same device measured again at SRI after a few days showed higher resistance initially and a steady state lower resistance with time. These variations clearly indicate that the polymer is being doped from the environment. Therefore, encapsulation will be needed for reliable device performance, which could be accomplished in future versions.

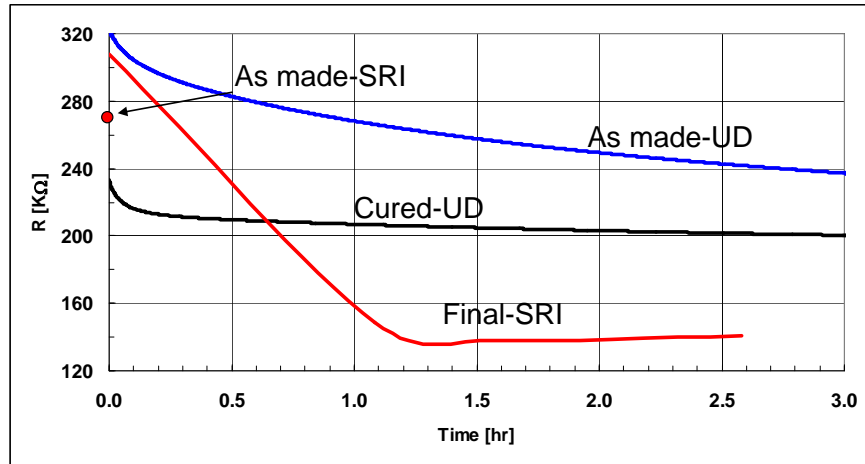


**Figure 4: Measured change in electrical resistance with time.**

Finally, we measured the LSMO device’s magnetic response and the measured change in MRI and plotted them as a function of magnetic field sweep in Figure 5. Since the measurements are carried out over a period of ~3 hours, the base resistance changes with time (as described above). More important, the periodic oscillation in MR associated with spin precession with a period of about 10 mG (0.001 mT) is not observed. If the room temperature magnetization and spin polarization of the LSMO contact is high, then the change in MR will be much higher than the noise inherent in polymer devices. Currently the signal, if any, is overwhelmed by noise, as



seen in Figure 5. The magnetization at room temperature is very small, owing to low  $T_c$ , and consequently, smaller spin polarization. Further, the sandwiched devices appear to have a poorer interface, resulting in diode-like, rather than ohmic, behavior. The lack of high spin injection at room temperature along with the effect of poorer interface on local measurements makes the LSMO devices not useful for room temperature magnetic sensing devices.

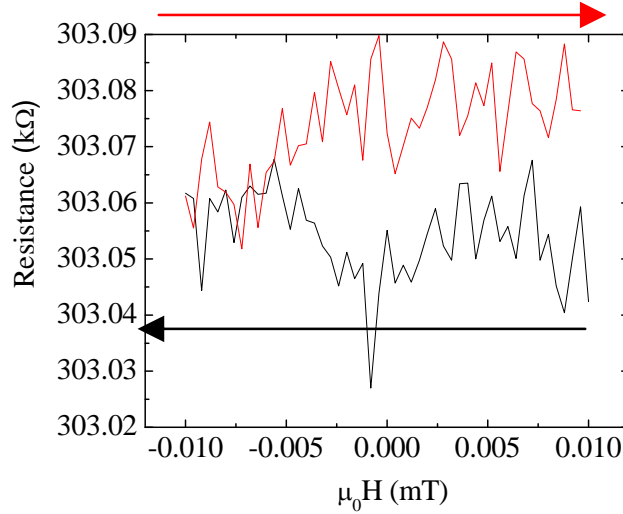


**Figure 5: Measured magnetoresistance at room temperature.**

## 5. Nonlocal CFAS Devices and Results

We have selected another FM material— $\text{CoFe}_{50}\text{Al}_{25}\text{Si}_{25}$  or CFAS—that has been demonstrated to have larger magnetization and coercive field and predicted to be half-metallic at room temperature. The Curie temperature is estimated to be in excess of 1000 K, and magnetization is shown to be relatively independent of temperature between 4 K and 300 K. All these features are expected to increase the magnetic sensing signal. For reduction in noise, we chose a nonlocal device as shown schematically in Figure 6. The terminals 1 (T1) through 4 (T4) are CFAS lines (in the  $z$  direction) on an STO substrate with carefully chosen widths ( $w_i$ ) and separated by selected distances ( $d_{ij}$ ). The polymer is drop-cast on CFAS lines. The CFAS contacts are magnetized. A constant current is supplied between T1 and T2. Depending on the magnetization of T2, charge carrier spins (parallel to the magnetization) accumulate under T2 and diffuse toward T3 and T4. In a steady-state distribution of spins, the potential measured between T3 and T4 depends on the density of carriers with spins parallel to their respective contact magnetization at T3 and T4. Since this is an open circuit voltage, no charge transport between T3 and T4 takes place. Consequently, the interface issues no longer contribute to noise. This material and design thus potentially increases the signal and decreases noise, thus likely to enable high sensitivity room temperature operation.

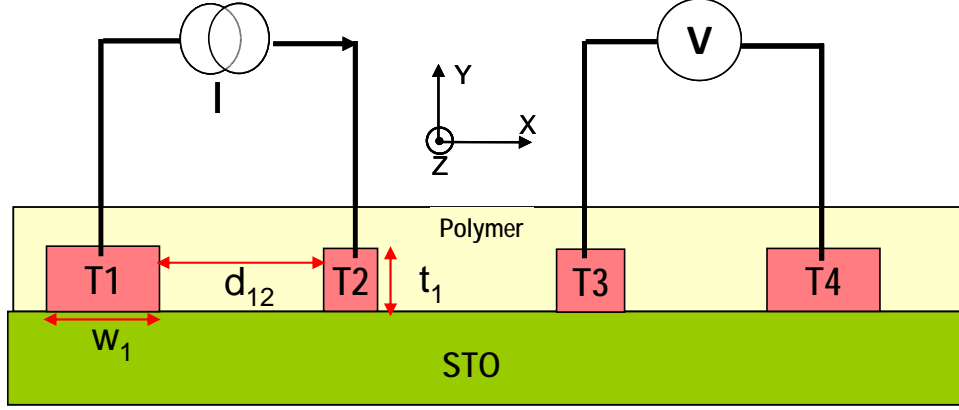


**Figure 6: Schematic nonlocal CFAS device.**

CFAS was grown at ASU by using pulsed laser deposition in one-step and two-step methods. In the one step method, the material is grown at high temperature ( $T_g$ ) for improved properties. In the two-step method, the layer is first grown at room temperature, followed by high-temperature anneal ( $T_a$ ). Several samples were grown, and magnetization as a function of magnetic field was measured systematically for various values of  $T_g$  and  $T_a$ . Figure 7 shows the measured coercive field ( $H_c$ ) and magnetization density ( $M_s$ ) of the samples grown by the one-step (blue line) and two-step (red line) methods.

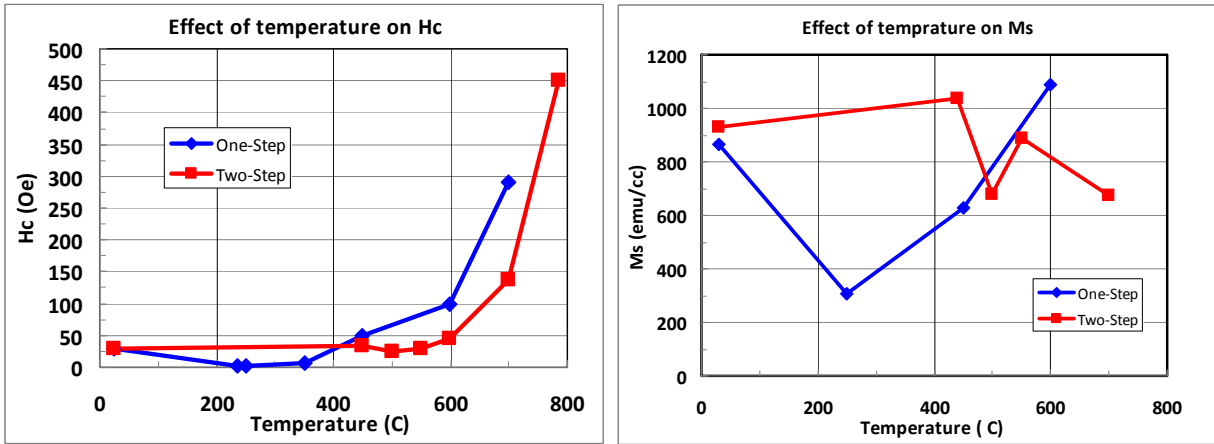


**Figure 7: Measured magnetic properties of CFAS layers at room temperature.**

In Figure 7, the temperature on the x-axis denotes  $T_g$  for the one-step and  $T_a$  for the two-step approach. We see that the coercive field and magnetization consistently increase at higher temperature in the one-step method. While coercive field increases also in the two-step method, the magnetization shows some fluctuations with  $T_a$ . Although some reduction in  $M_s$  could result from inaccuracy in estimating the layer thickness of those samples, we can conclude that higher

temperature anneal ceases to offer more advantage. We then measured magnetization as a function of magnetic field at various temperatures (4 K to 300 K); the results are shown in Figure 8. We see that the coercive field (the field at which magnetization is zero, or the x-axis intersection) changes slightly with temperature. Most important, the magnetization (the value at zero magnetic field, or the y-axis intersection) changes very little when the temperature is changed. Unlike LSMO, this material does not lose its magnetic (spin) properties at room temperature.

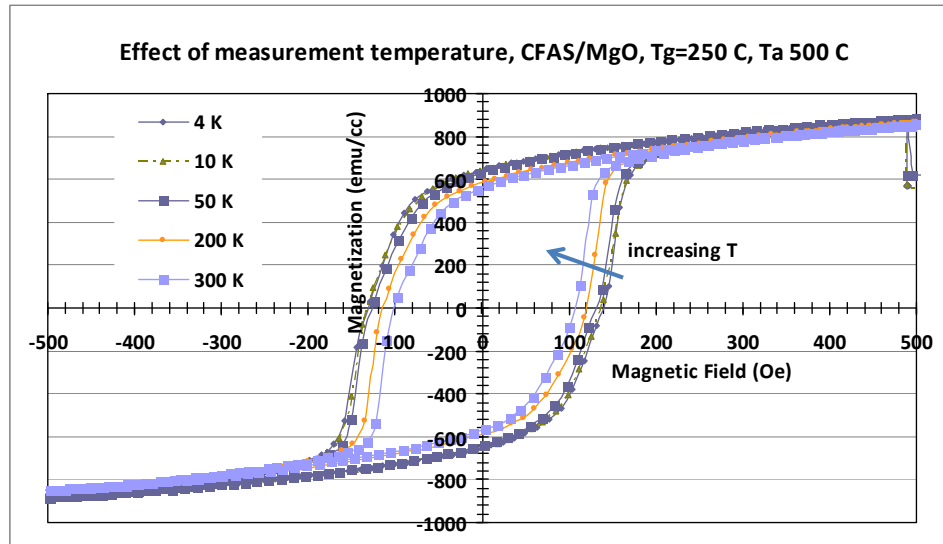


Figure 8: Field-magnetization curve for various sample temperatures.

We also measured electrical and magnetic resistivity of CFAS layers. The electrical resistivity is small ( $\sim 60 \mu\Omega\text{-cm}$ ) and changes very little with temperature as shown in Figure 9. The low resistivity confirms its metallic state, and the temperature independence implies that the layer is

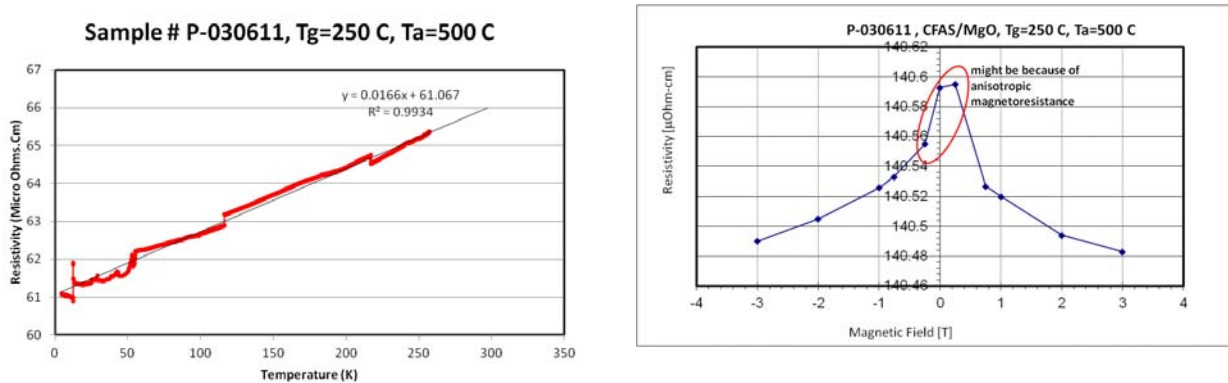


Figure 9: Measured electrical- and magnetoresistance

polycrystalline. The magnetoresistance is also very small ( $\sim 140 \mu\Omega\text{-cm}$ ) and is nearly independent of the magnetic field (about 0.1 W change with 3T of magnetic field).

We have just begun to fabricate the planar 4-terminal device using lithographic methods and identified PEDOT or MEH-PPV as the appropriate polymer material for spin injection. The fabrication is in progress.

We have further measured spin polarization,  $p$ , in CFAS at room temperature using the Andreev reflection technique. Systematic studies have not yet been performed. The preliminary data indicate that  $p$  is large and increases from 0.4 to 0.6 with an increase in  $T_g$  or  $T_a$ . The polarization value extracted from electrical data in the literature indicates that a much higher value of  $\sim 0.91$  is possible in DC magnetron-grown CFAS. As a parallel study, we have thus initiated CFAS growth by DC magnetron and will study the systematic change of  $p$  with  $T_g$ .

## 6. Conclusions

In conclusion, we have completed fabrication and testing of local LSMO devices and their usability for magnetic sensing. We found that the magnetization and spin polarization of LSMO at room temperature are not large enough to overcome the noise issues associated with sandwiched polymer devices. To address the issues of higher signal and lower noise, we have pursued the growth of a new material, CFAS, which has demonstrated high magnetization, high coercive field, low resistance, and medium-high spin polarization. Our material has the highest spin polarization demonstrated in any material in the literature, and efforts to increase spin polarization further with DC magnetron growth is under way. We have also started fabricating nonlocal magnetic sensor devices with our current CFAS layers. The results of our studies will be summarized and presented at the forthcoming ONR review in August 2011.